Chemical Engineering Journal 160 (2010) 199–206

Contents lists available at ScienceDirect

Chemical Engineering Journal

journal homepage: www.elsevier.com/locate/cej

Determination of optimum operating parameters for Acid Yellow 36 decolorization by electro-Fenton process using BDD cathode

K. Cruz-González, O. Torres-López, A. García-León, J.L. Guzmán-Mar, L.H. Reyes, A. Hernández-Ramírez, J.M. Peralta-Hernández *

Universidad Autónoma de Nuevo León, Facultad de Ciencias Químicas-CELAES, Pedro de Alba s/n, Cd. Universitaria, San Nicolás de los Garza, NL, C.P. 66400 México, Mexico

ARTICLE INFO

Article history:
Received 22 December 2009
Received in revised form 17 March 2010
Accepted 18 March 2010

Keywords:
Acid Yellow 36
Decolorization
Response surface methodology
Electro-Fenton
Boron-doped diamond electrodes
Wastewater treatment

ABSTRACT

The aim of this work was to apply an experimental response surface methodology (RSM) to optimization of the Acid Yellow 36 (Ay 36) decolorization procedure the electro-Fenton process (EFP) using boron-doped diamond (BDD) electrodes. RSM was used for the evaluation of different operation parameters, process modelling, optimization study, and model prediction analysis. Optimization of the electro-Fenton process for decolorization of 60 mg L^{-1} of synthetic azo dye solution was analyzed using a central composite design (CCD) in RSM. The response variable for the experimental design was a percentage of the color removal. The three considered factors, at two different levels, were current density (j = 8 and 23 mA/cm^2), catalytic Fe^{2+} concentrations (0.1 and 0.3 mmol L^{-1}), and electrolysis time (10 and 50 min). According to RSM, the optimum operation conditions were Fe^{2+} = 0.24 mmol L^{-1}, j = 23 mA/cm^2, and t = 48 min. The maximal decolorization efficiency of 98% was achieved under these conditions.

1. Introduction

Synthetic dyes represent one of the largest groups of pollutants in wastewater released from industrial processes. The textile industry is an important sector that consumes large quantities of water and chemicals for dyeing processes. In general, the chemical reagents used in dyeing and finishing operations show a wide diversity of chemical structures and variable compositions of inorganic and organic compounds, which generate a serious problem when these effluents are discharged to the environment [1]. Synthetic dyes are extensively used for textile dyeing processes, and approximately 50% of these compounds are azo dyes [2]. These compounds are characterized by one or more azo groups in the chemical structure (–N=N–), which are responsible for the dye color, and the presence of functional groups such as $–NH_2$, –OH, $–CH_3$, and $–SO_3$ are responsible for the fixation of these dyes to fibers [3]. Most of the azo dyes are considered to be essentially non-degradable using common methods (physicochemical treatment, active sludge, or oxidative techniques) [3]. Therefore, the development of an efficient process is required to remove synthetic dyes from aqueous effluents.

The use of hydrogen peroxide (H_2O_2) may offer an efficient means of controlling dye pollution in aqueous media. H_2O_2 is still one of the most popular non-selective oxidizing agents used for the oxidation of organic pollutants to carbon dioxide [4]. Recently, several works have demonstrated that *in situ* electrochemical generation of H_2O_2 can be successfully used for water treatment of effluents [5–8]. In this approach, H_2O_2 is continuously supplied to the contaminated solution by a two-electron oxygen (O_2) reduction in an acidic medium according to the following reaction [9–11]:

$$O_2 + 2H^+ + 2e^- \rightarrow H_2O_2 \quad (1)$$

This electrochemical process (reaction (1)) has been tested using a wide variety of carbonaceous electrodes with high surface area, such as reticulated vitreous carbon, carbon felt, graphite, or O_2-difussion cathodes [5,6,11–16]. In the case of boron-doped diamond (BDD), not much is known about H_2O_2 electrogeneration. Recently, Michaud et al. [17] proposed H_2O_2 production during the anodic oxidation of water (reaction (2)):

$$2H_2O \rightarrow H_2O_2 + 2e^- + 2H^+ \quad (2)$$

However, the use of a BDD cathode for H_2O_2 generation by O_2 reduction has not yet been tested.

The most common application of H_2O_2 in environmental applications involves addition of iron (Fe^{2+}) to an acidic solution to improve the oxidizing power of H_2O_2 to form free hydroxyl radicals ($^{\bullet}OH$) via the Fenton process, according to the following reaction [18–21]:

$$Fe^{2+} + H_2O_2 \rightarrow Fe^{3+} + {}^{\bullet}OH + {}^{-}OH \quad (3)$$

* Corresponding author. Tel.: +52 8183294000x6288.
E-mail address: juanperal@yahoo.com.mx (J.M. Peralta-Hernández).

1385-8947/$ – see front matter © 2010 Elsevier B.V. All rights reserved.
doi:10.1016/j.cej.2010.03.043

This method is denoted as the electro-Fenton process (EFP) and is included in the commonly used electrochemical advanced oxidation processes (EAOP) for removal of persistent organic pollutants from wastewater [22,23]. The reason for combining electrochemical H_2O_2 generation and the Fenton treatment is to improve the oxidation capacities of the two individual processes into a coherent and synergetic system [24].

EFP involves sequential pathways generating the $^{\bullet}OH$ and hydroperoxyl ($HO_2^{\bullet}$) free species that act in the reaction. According to Vatanpour et al. [25], the free radical mechanism consists of the following reactions:

$$^{\bullet}OH + H_2O_2 \rightarrow H_2O + HO_2^{\bullet} \quad (4)$$

$$Fe^{3+} + HO_2^{\bullet} \rightarrow Fe^{2+} + H^+ + O_2 \quad (5)$$

$$Fe^{2+} + HO_2^{\bullet} \rightarrow Fe^{3+} + HO_2^- \quad (6)$$

$$Fe^{2+} + {}^{\bullet}OH \rightarrow Fe^{3+} + OH^- \quad (7)$$

The $^{\bullet}OH$ is a strong oxidant with a standard potential of 2.8 V vs. NHE (pH 0) that is capable of destroying most of the organic matter present in water. In this context, EFP has been tested for decolorization of different azo dyes, such as Orange II, Azobenzene, p-Methyl Red, Methyl Orange, Direct Yellow 52 [26], and other dyes [27,28].

The use of experimental design methodology to optimize operating conditions that affect the azo dye decolorization efficiency by means of EFP has not been evaluated. This methodology has been explored to optimize wastewater treatment using other techniques. Fernández et al. [29] studied the variation of pH and H_2O_2 addition effects on the decolorization and mineralization of azo dye Orange II using heterogeneous photocatalysis (UV/TiO_2); they fit the optimal values of Orange II degradation using response surface methodology. Pérez-Moya et al. [30] proposed a multivariate experimental design for the treatment of 2-chlorophenol using a Fenton reagent under light irradiation. A factorial experimental design was established to assign each variable a weight in total organic carbon (TOC) removal. In 2007, Körbahti [31] carried out electrochemical treatment of three reactive dyes using iron electrodes in the presence of NaCl. This study was optimized using response surface methodology (RSM). In another report, Abdessalem et al. [32] applied an experimental design methodology to optimize the EFP. In this work, they evaluated the effect of selected experimental conditions, such as initial concentration, current density, and processing time, on the degradation and mineralization rate of the herbicide chlortoluron. The photocatalytic treatment of indole in the presence of titanium dioxide was optimized by Merabelt in 2009 by applying an experimental design methodology [33]. The effect of indole concentration, UV intensity, and stirring speed was studied in this work. Recently, Körbahti and Rauf [34] applied the response surface methodology to determine the optimum operation conditions for carmine decolorization using UV/H_2O_2 treatment. In this context, they found that carmine degradation was effected by carmine concentration, H_2O_2 concentration, pH, and reaction time.

In light of these approaches, the objective of this work was to apply RSM to optimize several operating conditions (current density, iron concentration, and electrolysis time) that have significant effects on the decolorization efficiency of azo dye Acid Yellow 36 (Ay 36) by EFP using a BDD cathode to produce H_2O_2. Finally, a verification study of the analysis was executed using the optimum operation conditions obtained from the experimental design RSM of the azo dye decolorization and degradation.

2. Materials and methods

2.1. Experimental

Chemicals used in this work, such as sulfuric acid (H_2SO_4), sodium sulfate (Na_2SO_4), and ferrous sulfate ($FeSO_4{\cdot}7H_2O$), were purchased from J.T. Baker as ACS reagent grade and used as received without further purification. Titanium (IV) sulfate [$Ti(SO_4)_2$] was purchased from Aldrich Co. and the azo dye, Acid Yellow 36 (Ay 36, $C_{18}H_{15}N_3O_3S$, λ_{max} = 437 nm), industrial grade, was supplied by Orion Co. Diamond (BDD) electrode was provided by Adamant-Technologies (Switzerland).

2.1.1. Dye solution preparation

An accurately weighed quantity of the Ay 36 dye was dissolved in distilled water to prepare the stock solution (100 mg L^{-1}). Experimental solutions of the desired concentration (60 mg L^{-1}) were obtained by successive dilution. The synthetic textile dye wastewater solution was prepared in accordance with literature reports [26,31], where dye concentrations in textile wastewater ranged from 10 to 200 mg L^{-1}.

2.1.2. Electrochemical setup

The experiments were conducted at room temperature in an open, undivided, and cylindrical glass cell of 100 mL capacity and were performed in galvanostatic mode at three current densities (j = 8, 15, and 23 mA/cm^2). A BDD plate (geometric area, 2 cm^2) was used as a cathode and platinum was used as an anode (geometric area, 4 cm^2). The gap between electrodes was 2.5 cm. All experiments were carried out in acidic solution of sulfates (0.05 M) adjusted to pH 3 with sulfuric acid. Prior to electrolysis, air was bubbled through the setup for 30 min to saturate the solution. Different iron concentrations in the form of ferrous sulfate solution (0.1, 0.2, and 0.3 mmol L^{-1}) were added to evaluate the effect on dye oxidation rate via EFP.

2.1.3. Hydrogen peroxide evaluation

Evaluation of H_2O_2 accumulation in the system was carried out by testing of oxygen reduction (O_2) in a saturated air solution of 0.05 M Na_2SO_4 at pH 3. The H_2O_2 concentration was determined using the $Ti(SO_4)_2$ titration method and spectrophotometric analysis at λ = 407 nm [35].

2.1.4. Analytic procedure

At given time intervals, aliquots were sampled and analyzed by recording variations of the dye absorption band at 437 nm for Ay 36 in the UV–vis spectra (Fig. 1), using a Lambda 12 spectrophotometer (Perkin Elmer Co.).

The degradation of Ay 36 was monitored by high performance liquid chromatography (HPLC) analysis, using a Perkin Elmer Series 200 equipped with a UV/vis Detector. A reverse phase C-18 Perkin Elmer (5 μm, 250 mm × 4.6 mm) column was used in the experiments. The volume of injection was 20 μL. The column was eluted with a mixture of ammonium acetate 10 mmol L^{-1}/acetonitrile 70:30 (v/v) with a flow rate 0.8 mL min^{-1}. Detection was performed at 277 nm [22].

2.1.5. Response surface methodology (RSM)

RSM was applied for the experiments. RSM is essentially a particular set of mathematical and statistical tools for designing experiments, building models, evaluating the effects of operation conditions, and most importantly, for searching the optimum values of factors to predict target response [31,36,37]. In this context, RSM is an important derivation of experimental design and is a critical technique for development of a new process or products, as well as optimization of their performance [31,36,37]. RSM allows

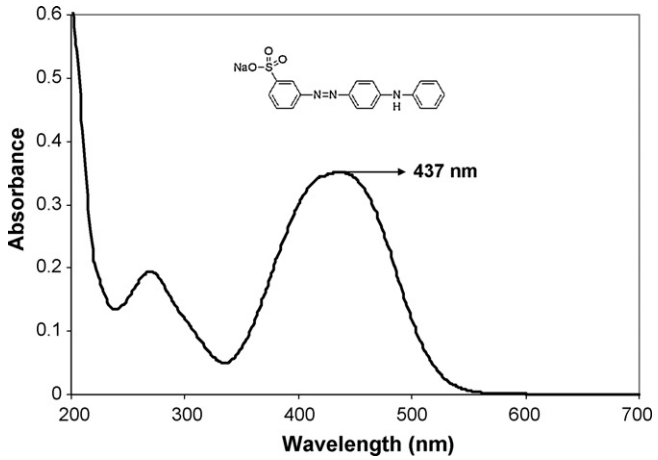

Fig. 1. Absorption spectra of Acidic Yellow 36 (60 mg L^{-1}) before treatment. Insert corresponds to the azo dye structure.

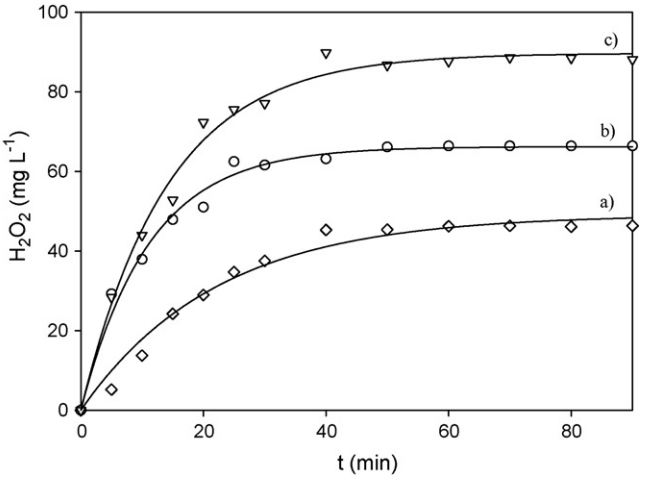

Fig. 2. Accumulation of H_2O_2 in 0.05 M of Na_2SO_4 solution at pH 3 under different current densities using BDD cathode. (a) 8 mA/cm^2, (b) 15 mA/cm^2, and (c) 23 mA/cm^2.

for a considerable reduction in the number of experiments and easy interpretation because with the experimental design, is it possible to study a large number of factors and detect the possible interactions between them [32].

By using the experimental design methodology, it was possible to design and optimize the decolorization efficiency of Ay 36 using EFP, estimate the linear interaction effects of the factors, and construct a prediction model for the response. The independent factors were current density, Fe^{2+} concentration, and electrolysis time.

A central composite design (CCP) was used in the RSM, and the current and coded factors and their levels are shown in Table 1 for the Ay 36 decolorization. The data were evaluated by analysis of variance (ANOVA) and using Design Expert Version 6.0.1 (StatEase, USA). The design was performed with 45 experiments: eight factorial points (three replicates), three central points, and six axial points (three replicates).

Table 1
Experimental design of Ay 36 decolorization by means of EFP.

Independent variable	Factor	−1	Coded levels 0 Actual levels	+1
Current density (mA/cm^2)	A	8	15	23
Catalytic Fe^{2+}concentration (mM)	B	0.1	0.2	0.3
Electrolysis time (min)	C	10	30	50

3. Results and discussion

3.1. H_2O_2 generation on the BDD cathode

The capacity of the system for electrochemical generation of H_2O_2 by O_2 reduction (reaction (1)) on a BDD cathode was studied by sampling the solution and determining the concentration of the accumulated H_2O_2 using spectrophotometric analysis. Fig. 2 shows

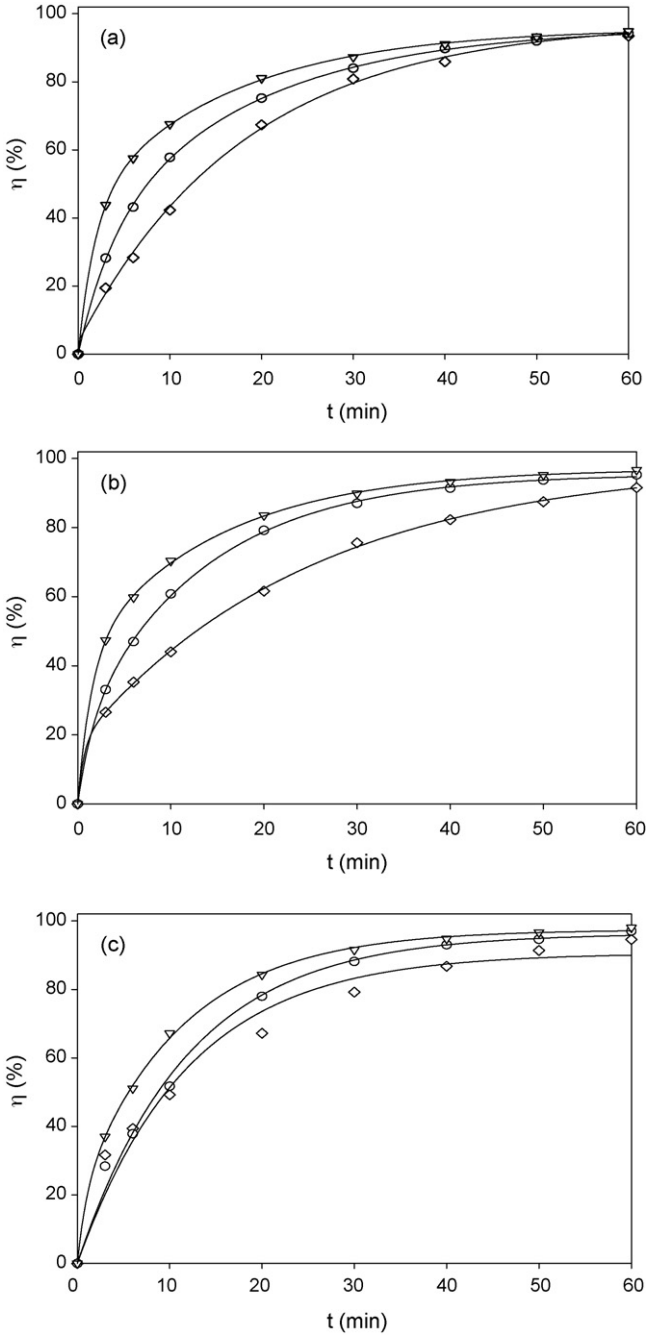

Fig. 3. Decolorization efficiency of azo dye Ay 36 (C_0 = 60 mg L^{-1}) in 0.05 M of Na_2SO_4 solution at pH 3 during the electro-Fenton process using a BDD cathode in the presence of different Fe^{2+} concentrations: (◊) 0.1 mmol L^{-1}, (○) 0.2 mmol L^{-1}, and (▽) 0.3 mmol L^{-1}, and under different current densities: (a) 8 mA/cm^2, (b) 15 mA/cm^2, and (c) 23 mA/cm^2.

Table 2
Evaluation of kinetic constants for Ay 36 decolorization using EFP.

$[Fe^{2+}]$ (mM)	K (min^{-1})
$j = 8\ mA/cm^2$	
0.1	5.02×10^{-2}
0.2	5.48×10^{-2}
0.3	5.51×10^{-2}
$j = 15\ mA/cm^2$	
0.1	4.19×10^{-2}
0.2	5.99×10^{-2}
0.3	6.63×10^{-2}
$j = 23\ mA/cm^2$	
0.1	4.60×10^{-2}
0.2	5.79×10^{-2}
0.3	7.00×10^{-2}

the concentration of electrochemically generated H_2O_2 as a function of time for three current densities applied. Curve a corresponds to the cathodic current density $j = 8\ mA/cm^2$, curve b is obtained with $j = 15\ mA/cm^2$, and curve c corresponds to $j = 23\ mA/cm^2$. In all cases, it was observed that the peroxide level increased during the first 40 min of electrolysis and then leveled off at constant values of 46, 66, and 88 mg L^{-1}, for curves a, b and c, respectively. This behavior can be explained by considering that, in the steady state, the rate of production of H_2O_2 is simultaneously balanced by its rate of decomposition, both at the anode and perhaps homogeneously [35,38]. From estimates of the initial slopes in Fig. 2, it appears that the net current efficiency for peroxide production is about 10% when its level in solution is negligible, and it falls off from there.

3.2. Decolorization efficiency of Ay 36 by EFP and kinetic parameters

The next set of tests involved the continuous electrochemical generation of H_2O_2 in the presence of ferrous ions, i.e., the EFP. The

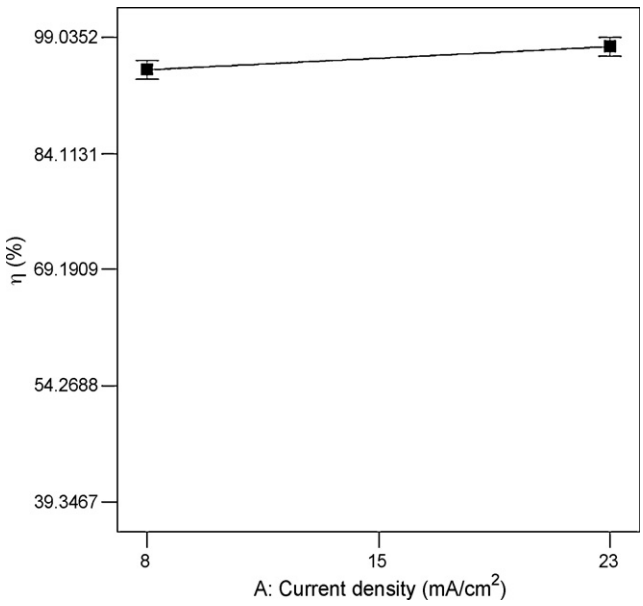

Fig. 4. One factor plot of current density for Ay 36 decolorization efficiency.

decolorization efficiency (η) is defined as:

$$\eta\ (\%) = \frac{C_0 - C}{C_0} \times 100 \quad (8)$$

where C_0 and C are Ay 36 concentration at initial time and given time t, respectively [3]. Decolorization efficiency experiments were carried out at each cathodic current density proposed in Section 3.1, and at three levels of ferrous sulfate, 0.1, 0.2, and 0.3 mmol L^{-1}. Fig. 3 depicts the influence of current density and Fe^{2+} on the decolorization kinetic. The efficiency of EFP was examined by treating a dye solution containing 60 mg L^{-1} of Ay 36 at pH 3. As can be seen in Fig. 3a for $j = 8\ mA/cm^2$, the decolorization rate increased

Table 3
Experimental design results.

Experimental number	Coded level of factors			Observed percentage of removals			Average
	A	B	C	Replication 1	Replication 2	Replication 3	
1	−1	−1	−1	42.32	39.35	41.69	41.12
2	1	−1	−1	49.20	45.09	45.63	46.64
3	−1	+1	−1	67.55	71.34	61.31	66.73
4	+1	+1	−1	67.14	65.61	70.42	67.72
5	−1	−1	+1	92.76	89.04	85.93	89.24
6	+1	−1	+1	91.37	93.04	92.65	92.35
7	−1	+1	+1	93.25	96.10	90.69	93.35
8	+1	+1	+1	96.64	96.58	97.11	96.78
9	−1	0	0	83.96	87.22	84.27	85.15
10	+1	0	0	88.11	88.90	83.86	86.96
11	0	−1	0	75.23	75.60	74.53	75.12
12	0	+1	0	93.27	89.83	91.40	91.50
13	0	0	−1	61.71	60.79	61.06	61.18
14	0	0	+1	94.23	93.73	94.68	94.21
15	0	0	0	87.41	86.97	87.93	87.44

Table 4
ANOVA results of the quadratic model of Ay 36 decolorization using EFP.

Variation source	Sum of square	Degree of freedom	Mean square	*F*-Value	*P*-Value
Model	13,301.50	6	2216.92	421.99	<0.0001
Residual	199.64	38	5.25	103.97	
Lack of fit	52.63	8	6.58	1.34	0.2614
Pure error	147.02	30	4.90		
Total	13,501.15	44			

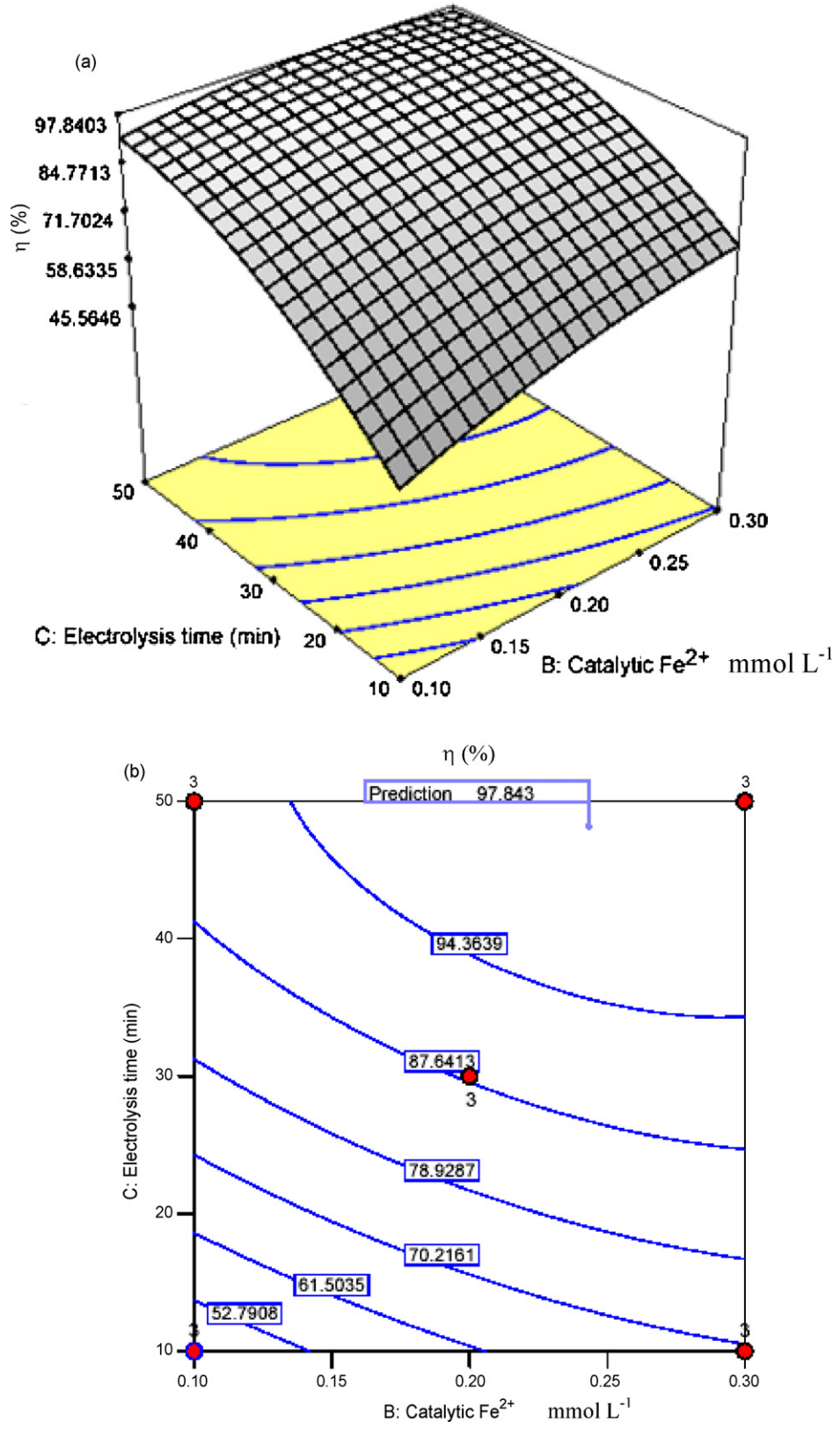

Fig. 5. Effect of electrolysis time and Fe^{2+} concentration interaction on Ay 36 decolorization efficiency: (a) response surface plot and (b) contour plot.

as Fe^{2+} was added to the solution, reaching a maximum increase with an Fe^{2+} concentration of 0.3 mmol L^{-1}; Ay 36 decolorization of 94% was achieved after 60 min of electrolysis. This enhancement in oxidation power is noticeable at $j = 15$ mA/cm^2 (Fig. 3b) suggesting that the process was improved with the addition of 0.3 mmo L^{-1} of Fe^{2+} wherein a decolorization efficiency of 97% was achieved. However, the result was similar with 0.2 mmol L^{-1} of iron concentration; the decolorization efficiencies showed almost overlapped curves between 30 and 60 min. Fig. 3c corresponds to the assay results with $j = 23$ mA/cm^2, and here it was possible to observe that

Ay 36 decolorization efficiency was very fast, quickly reaching 99% with 0.3 mmol L^{-1} of Fe^{2+}.

According to this trend, decolorization of Ay 36 was achieved over shorter times with an increase in current density and Fe^{2+} concentration; in this context, the apparent constant rate of the oxidation reaction was given by the following reaction:

$$\text{Ay 36} + {}^{\bullet}\text{OH} \rightarrow \text{decolorization} + \text{oxidation products} \quad (9)$$

and can be determined by assuming a stationary state for the concentration of free hydroxyl radicals [2].

The kinetics of the electro-Fenton reaction can be fitted using apparent first-order kinetics. Most kinetic studies of decolorization and aromatic content removal of azo dyes assisted by the Fenton process can be described by a first-order rate equation [39]. In this study, the rate of decolorization of Ay 36 (λ_{max} = 437 nm) followed the next equation:

$$\ln\frac{C_0}{C} = k_1 t \quad (10)$$

where k_1 is the apparent first-order reaction rate constant, t is the reaction time, and C_0 and C are the initial and final concentration values of the dye solution, respectively. The results are shown in Table 2. From this table, the best experimental conditions without RSM analysis for Ay 36 decolorization by EFP occurred with the addition of 0.3 mmol L^{-1} of Fe^{2+}, 23 mA/cm^2 current density, and 60 min electrolysis time, achieving a kinetic constant of 7.0×10^{-2} min^{-1}.

3.3. Experimental design and optimization of operation conditions in the decolorization kinetics of Ay 36 by means of EFP

In light of the experimental design results (Table 3), the quadratic regression model that established the correlation between the decolorization efficiency of Ay 36 and the independent factors was found to be:

$$\eta(\%) = 86.57 + 1.49 * A + 7.16 * B + 18.25 * C - 3.35 * B^2 - 8.96 * C^2 - 4.77 * B * C \quad (11)$$

Table 4 shows the ANOVA results from this model, where the model's F-value of 421.96 implies that the model was significant for Ay 36 dye decolorization. The values of $P > F$ less than 0.0500 indicate that model terms are significant, whereas values greater than 0.1000 are not significant. For this model, $P > F$ is less than 0.0001, indicating that term was significant in this model. A positive effect of a factor means that the response is improved when the factor level increases and a negative effect of the factor means that the response is not improved when the factor level increases. The positive effects were the individual factors of electrolysis time, Fe^{2+} concentration, and current density, in this order. The negative effects were the quadratic factors of electrolysis time and Fe^{2+}, as well as the double interaction between Fe^{2+} and electrolysis time.

3.4. Response analysis for Ay 36 decolorization efficiency

The current density factor was significant at the 8 mA/cm^2 significance threshold, and the one factor plot showed that the decolorization efficiency improved when the factor increased of 8 at 23 mA/cm^2 (Fig. 4) and holding the other factors constant.

A study of the response surface and contour plots provided an easy method for optimization of the efficiency of the electro-Fenton treatment. The response surface plot for Ay 36 decolorization is shown in Fig. 5a, when the current density was established at 23 mA/cm^2 as observed in Fig. 4. The semispherical response surface of decolorization slightly increased with increasing Fe^{2+} concentration, from 0.15 to 0.24 mmol L^{-1}, and then decreased above 0.3 mmol L^{-1}. A similar trend was also observed for electrolysis time but the curvature was sharp, which means that the decolorization quickly increased with increases in the electrolysis time from 10 to 48 min, and then slightly decreased from 48 to 50 min. In the scope of the results, the maximum value of decolorization percentage of Ay 36 was determined to be 97.8% at 0.24 mmol L^{-1} of Fe^{2+} and 48 min (Fig. 5b).

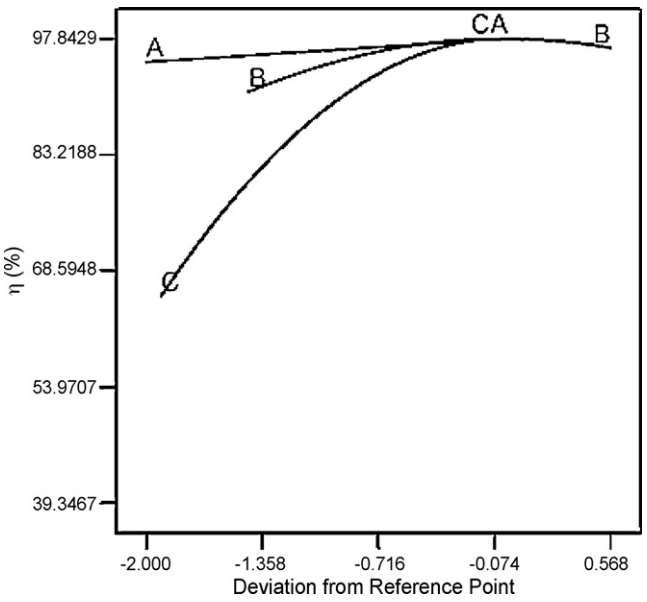

Fig. 6. Perturbation plot for Ay 36 decolorization.

In the perturbation plot, Fig. 6 shows the effects when all factors at the optimum experimental conditions in the design space are compared. The perturbation plot assists in comparison of the effects of all factors at a particular point in the design space; when the factor curvature is sharper, the factor effect is more important to the response. The plot was obtained for 0.24 mmol L^{-1} Fe^{2+}, 48 min of electrolysis time, and 23 mA/cm^2. Fig. 6 shows that the response of Ay 36 decolorization was very sensitive to the electrolysis time, followed by Fe^{2+} concentration, and finally, by current density.

3.5. Verification study

To confirm the adequacy of the model, three sets of assays were randomly carried out at optimum conditions to obtain a maximum Ay 36 decolorization result. Fig. 7 presents the experimental results under the optimum conditions as compared with the decolorization efficiency by means of EFP without RSM analysis. As can be seen in this Fig., the decolorization efficiency of Ay 36 was close to 98%, and the kinetic constant value was 9.75×10^{-2} min^{-1} under optimal operating conditions as compared with the kinetic constant for EFP without RSM analysis (7.0×10^{-2} min^{-1}). The experimental error of less than 1.0% indicated that the proposed model was adequate for prediction of the optimum value of decolorization efficiency in the range of factors studied.

Additionally, degradation behavior of Ay 36 was evaluated by RP-HPLC using the experimental conditions obtained by the response surface analysis method. The decay of Ay 36 concentration was followed under reversed-phase HPLC conditions (as indicated in Section 2). Ay 36 eluted at retention time t_r = 10.77 min. The evolution of Ay 36 by EFP under non-optimized conditions (t = 60 min, 0.3 mmol L^{-1} Fe^{2+}, j = 23 mA/cm^2, $k = 7.0 \times 10^{-2}$ min^{-1}) and optimized conditions (t = 48 min, 0.24 mmol L^{-1} Fe^{2+}, 23 mA/cm^2, $k = 9.75 \times 10^{-2}$ min^{-1}) is shown in Fig. 8. As can be seen, the concentration of Ay 36 by EFP under non-optimized conditions (◊) slowly

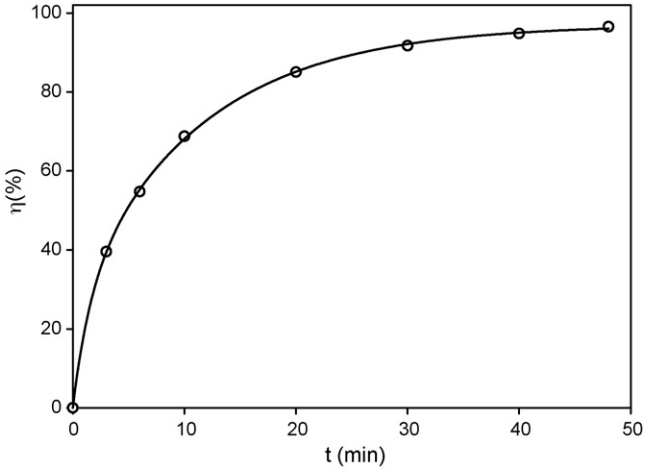

Fig. 7. Decolorization of Ay 36 under optimum conditions by CCD design.

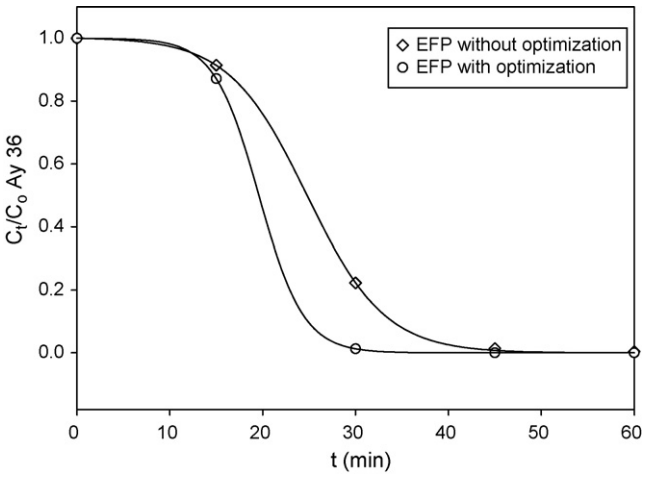

Fig. 8. Degradation of Ay 36 in acidic solution (pH 3) by EFP under non-optimized conditions (◊), and optimized conditions (○).

decreased at the initial stage of electrolysis and the time necessary to observe a complete disappearance of Ay 36 was close to 45 min. On the other hand, under the optimized conditions (○) the concentration Ay 36 rapidly diminished and the azo dye was completely degraded after 30 min of treatment. These results indicated the suitability of the model. The RSM was successfully applied to optimize the EFP of Ay 36.

4. Conclusion

The decolorization of Ay 36 in acidic aqueous medium was analyzed by applying EFP based on the use of a BDD cathode to effectively produce H_2O_2 in the medium via oxygen reduction. Under the central composite design of RSM, the optimum conditions of Fe^{2+} = 0.24 mmol L^{-1}, j = 23 mA/cm^2, and t = 48 min were chosen to achieve 97.8% Ay 36 decolorization. This result indicated the suitability of the proposed model showing an important enhancement of the kinetic constant value and the degradation percent of Ay 36 compared to the results achieved under non-optimized conditions.

Acknowledgements

Financial support from CONACyT (Grant 25602), PROMEP/103.5/09/4909, and UANL-PAICyT (IT 156-09) is gratefully acknowledged. We also acknowledge Dr. Sergio Fernández, Dean of Chemistry Science School UANL for his support to our research group.

References

[1] T. Robinson, G. McMullan, R. Marchat, P. Nigam, Remediation of dyes in textile effluent: a critical review on current treatment technologies with a proposed alternative, Bioresour. Technol. 77 (2001) 247–255.
[2] S. Hammami, N. Bellakhal, N. Oturan, M.A. Oturan, M. Dachraoui, Degradation of acid orange 7 by electrochemicaly generated •OH radicals in acidic aqueous medium using a boron-doped diamond or platinum anode: a mechanistic study, Chemosphere 73 (2008) 678–684.
[3] D. Melgoza, A. Hernández-Ramírez, J.M. Peralta-Hernández, Comparative efficiencies of the decolourisation of methylene blue using Fenton's and photo-Fenton's reactions, Photochem. Photobiol. Sci. 8 (2009) 596–599.
[4] C. Badellino, C. Arruda Rodrigues, R. Bertazzoli, Oxidation of pesticides by in situ electrogenerated hydrogen peroxide: study for the degradation 2,4-dichlorophenoxyacetic acid, J. Hazard. Mater. B 137 (2006) 856–864.
[5] J.S. Do, C.P. Chen, In situ oxidative degradation of formaldehyde with hydrogen peroxide electrogenerated on the modified graphites, J. Appl. Electrochem. 24 (1999) 936–942.
[6] C.P. de Leon, D. Pletcher, Removal of formaldehyde from aqueous solutions via oxygen reduction a reticulated vitreous carbon cell, J. Appl. Electrochem. 25 (1995) 307–314.
[7] A. Alvarez-Gallegos, D. Pletcher, The removal of low levels of organics via hydrogen peroxide formed in a reticulated vitreous carbon cathode cell. Part 1. The electrosynthesis of hydrogen peroxide in aqueous acidic solutions, Electrochim. Acta 44 (1998) 853–861.
[8] A. Alvarez-Gallegos, D. Pletcher, The removal of low levels of organics via hydrogen peroxide formed in a reticulated vitreous carbon cathode cell. Part 2. The removal of phenols and related compounds from aqueous effluents, Electrochem. Acta 44 (1999) 2483–2492.
[9] E. Brillas, M.A. Baños, S. Camps, C. Arias, P.-L. Cabot, J.A. Garrido, R.M. Rodríguez, Catalytic effect of Fe^{2+}, Cu^{2+} and UVA light on the electrochemical degradation of nitrobenzene using an oxygen-diffusion cathode, New J. Chem. 28 (2004) 314–322.
[10] B. Gözmen, M.A. Oturan, N. Oturan, O. Erbatur, Indirect electrochemical treatment of bisphenol A in water via electrochemically generated Fenton's reagent, Environ. Sci. Technol. 37 (2003) 3716–3723.
[11] J.M. Peralta-Hernández, Y. Meas-Vong, F.J. Rodríguez, T.W. Chapman, M.I. Maldonado, L.A. Godínez, In situ electrochemical and photo-electrochemical generation of the Fenton reagent: a potentially important new water treatment technology, Water Res. 40 (2006) 1754–1762.
[12] E. Brillas, R. Sauleda, J. Casado, Degradation of 4 chlorophenol by anodic oxidation, electro-Fenton, photoelectro-Fenton, and peroxi-coagulation processes, J. Electrochem. Soc. 145 (1998) 759–765.
[13] M.A. Oturan, An ecologically effective water treatment technique using electrochemically generated hydroxyl radicals for in situ destruction of organic pollutants: application to herbicide 2,4-D, J. Appl. Electrochem. 30 (2000) 475–482.
[14] E. Brillas, J.C. Calpe, J. Casado, Mineralization of 2,4-D by advanced electrochemical oxidation processes, Water Res. 34 (2000) 2253–2262.
[15] E. Brillas, B. Boye, M.M. Dieng, General and UV-assisted cathodic Fenton treatments for the mineralization of herbicide MCPA, J. Electrochem. Soc. 150 (2003) 583–589.
[16] I. Sirés, J.A. Garrido, R.M. Rodríguez, P.L. Cabot, F. Centellas, C. Arias, E. Brillas, Electrochemical degradation of paracetamol from water by catalytic action of Fe^{2+}, Cu^{2+}, and UVA light on electrogenerated hydrogen peroxide, J. Electrochem. Soc. 153 (2006) D1–D9.
[17] P.A. Michaud, M. Panizza, L. Ouattara, T. Diaco, G. Foti, Ch. Comninellis, Electrochemical oxidation of water on synthetic boron-doped diamond thin film anodes, J. Appl. Electrochem. 33 (2003) 151–154.
[18] M.A. Oturan, N. Oturan, C. Lahitte, S. Trevin, Production of hydroxyl radicals by electrochemically assisted Fenton's reagent. Application to the mineralization of an organic micropollutant, pentachlorophenol, J. Electroanal. Chem. 507 (2001) 96–102.
[19] J.J. Aaron, M.A. Oturan, New photochemical and electrochemical method for the degradation of pesticides in aqueous media. Environmental applications, Turk. J. Chem. 25 (2001) 509–520.
[20] E. Brillas, I. Sirés, M.A. Oturan, Electro-Fenton process and related electrochemical technologies based on Fenton's reaction chemistry, Chem. Rev. 109 (2009) 6570–6631.
[21] E. Brillas, M.A. Baños, M. Skoumal, P.L. Cabot, J.A. Garrido, R.M. Rodríguez, Degradation of the herbicide 2,4-DP by anodic oxidation, electro-Fenton and photoelectro-Fenton using platinum and boron-doped diamond anodes, Chemosphere 68 (2007) 199–209.
[22] A. Özcan, Y. Şahin, A.S. Koparal, M.A. Outran, Electro-Fenton removal of the cationic dye basic blue 3 by using carbon felt cathode, J. Environ. Eng. Manage. 19 (2009) 267–275.
[23] N. Oturan, I. Sirés, M.A. Oturan, E. Brillas, Degradation of pesticides in aqueous medium by electro-Fenton and related methods. A Review, J. Environ. Eng. Manage. 19 (2009) 235–255.
[24] M. Panizza, G. Cerisola, Removal of organic pollutants from industrial wastewater by electrogenerated Fenton's reagent, Water Res. 35 (2001) 3987–3992.

[25] V. Vatanpour, N. Daneshvar, M.H. Rasoulifard, Electro-Fenton degradation of synthetic dye mixture: influence of intermediates, J. Environ. Eng. Manage. 19 (2009) 277–282.
[26] J.M. Peralta-Hernández, C.A. Martínez-Huitle, J.L. Guzmán-Mar, A. Hernández-Ramírez, Recent advances in the application of electro-Fenton and photoelectro-Fenton process for removal of synthetic dyes in wastewater treatment, J. Environ. Eng. Manage. 19 (2009) 257–265.
[27] Y.B. Xie, X.Z. Li, Interactive oxidation of photoelectrocatalysis and electro-Fenton for azo dye degradation using TiO_2–Ti mesh and reticulated vitreous carbon electrodes, Mater. Chem. Phys. 95 (2006) 39–50.
[28] E. Guivarach, S. Trevin, C. Lahitte, M.A. Oturan, Degradation of azo dye in water by electro-Fenton process, Environ. Chem. Lett. 1 (2003) 38–44.
[29] J. Fernández, J. Kiwi, J. Baeza, J. Freer, C. Lizama, H.D. Mansilla, Orange II photocatalysis on immobilised TiO_2 effect of the pH and H_2O_2, Appl. Catal. B: Environ. 48 (2004) 205–211.
[30] M. Pérez-Moya, M. Graells, L.J. del Valle, E. Centelles, H.D. Mansilla, Fenton and photo-Fenton degradation of 2-chlorophenol: multivariate analysis and toxicity monitoring, Catal. Today 124 (2007) 163–171.
[31] B.K. Körbahti, Response surface optimization of electrochemical treatment of textile dye wastewater, J. Hazard. Mater. 145 (2007) 277–286.
[32] A.K. Abdessalem, N. Oturan, N. Bellakhal, M. Dachraoui, M.A. Oturan, Experimental design methodology applied to electro-Fenton treatment for degradation of herbicide chlortoluron, Appl. Catal. B. Environ. 78 (2008) 334–341.
[33] S. Merabet, D. Robert, J.V. Weber, M. Bouhelassa, S. Benkhanouche, Photocatalytic degradation of indole in UV/TiO_2: optimization and modeling using the response surface methodology (RSM), Environ. Chem. Lett. 7 (2009) 45–49.
[34] B.K. Körbahti, M.A. Rauf, Determination of optimum operating conditions of carmine decoloration by UV/H_2O_2 using response surface methodology, J. Hazard. Mater. 161 (2009) 281–286.
[35] J.M. Peralta-Hernández, Y. Meas-Vong, F.J. Rodríguez, T.W. Chapman, M.I. Maldonado, L.A. Godínez, Comparison of hydrogen peroxide-based processes for treating dye-containing wastewater: decolorization and destruction of Orange II azo dye in dilute solution, Dyes Pigments 76 (2008) 656–662.
[36] R.H. Myers, D.C. Montgomery, Response Surface Methodology: Process and Product Optimization Using Design Experiments, 2nd ed., John Wiley and Sons, USA, 2002.
[37] D.C. Montgomery, Design and Analysis of Experiments, 4th ed., John Wiley and Sons, USA, 1996.
[38] A. Wang, J. Qu, J. Ru, H. Liu, J. Ge, Mineralization of an azo dye Acid Red 14 by electro-Fenton's reagent using an activated carbon fiber cathode, Dyes Pigments 65 (2005) 227–233.
[39] L. Núñez, J.A. García-Hortal, F. Torrades, Study of kinetic parameters related to the decolourization and mineralization of reactive dyes from textile dyeing using Fenton and photo-Fenton processes, Dyes Pigments 75 (2007) 647–652.